Intrinsic activity of oxygen evolution catalysts probed at single $CoFe_2O_4$ nanoparticles

Abdelilah El Arrassi[‡], Niclas Blanc[‡], Zhibin Liu[‡], Mathies V. Evers[‡], Georg Bendt[†], Sascha Saddeler[†], David Tetzlaff[‡], Darius Pohl[$,§], Christine Damm[§], Stephan Schulz[†], Kristina Tschulik*[,‡]

‡ Ruhr University Bochum, Faculty of Chemistry and Biochemistry, Analytical Chemistry II, Bochum, Germany

† University of Duisburg-Essen, Faculty of Chemistry and Center for Nanointegration Duisburg-Essen (CENIDE), Universitätsstraße 7, 45141 Essen, Germany

§ IFW Dresden, Helmholtzstraße 20, 01069 Dresden, Germany

$ Dresden Center for Nanoanalysis, TU Dresden, D-01062 Dresden, Germany

Supporting Information Placeholder

ABSTRACT: Identifying the intrinsic electrocatalytic activity of nanomaterials is challenging, as usually their characterization requires additives and binders whose contributions are difficult to dissect. Herein, we use nano impact electrochemistry as an additive-free method to overcome this problem. Due to the efficient mass transport at individual catalyst nanoparticles, high current densities can be realized. High-resolution bright-field transmission electron microscopy and selected area diffraction studies of the catalyst particles before and after the experiments provide valuable insights in the transformation of the nanomaterials during harsh oxygen evolution reaction (OER) conditions. We demonstrate this for 4 nm sized $CoFe_2O_4$ spinel nanoparticles. It is revealed that these particles retain their size and crystal structure even after OER at current densities as high as several $kA \cdot m^{-2}$. The steady-state current scales with the particle size distribution and is limited by the diffusion of produced oxygen away from the particle. This versatilely applicable method provides new insights into intrinsic nanocatalyst activities, which is key to the efficient development of improved and precious metal-free catalysts for renewable energy technologies.

Efficient development and characterization of electrocatalysts for multi-electron transfer reactions is important but difficult. To date IrO_2 and RuO_2 benchmark the list of oxygen evolution reaction (OER) catalysts, thanks to their excellent and long-term catalytic activity.[1,2] Due to their low supply and high price, it is highly important to identify alternative highly active low-cost OER electrocatalysts, based on earth-abundant elements. Transition metal oxides are promising candidates to meet these demands.[3] Due to their high surface-to-volume ratio and tunable electronic properties, nanomaterials are particularly favorable to enhance the performance of electrocatalysts. Yet, to date no routine exists, that allows measuring the *intrinsic* catalytic activity of such electrocatalysts. The common approach to test electrocatalytically active nanoparticles is done by ensemble studies, in which typically $>>10^3$ particles are mixed with conductive additives and binders, like carbon powder and Nafion®. These mixtures are then supported on an electrode and the overall electrochemical performance of this mixture is analyzed, prohibiting the identification of individual intrinsic particle activities.

The evaluation of precious metal-free OER catalysts is a particularly difficult challenge due to the highly oxidative potentials required to drive this multi-electron and multi-proton redox reaction, and the fact that catalyst-binder composites are analyzed to overcome the poor electronic conductivities of these materials. Accordingly, the electrochemically active surface area of these catalysts can neither be determined precisely, nor can overlying influences of the usually poor electrical conductivity of the catalysts precisely be dissected.

Here we demonstrate that single entity electrochemistry allows us to test nanocatalysts on an individual particle level and in the absence of additives obstructing the intrinsic catalyst properties. This is shown for spinel cobalt iron oxide ($CoFe_2O_4$) nanoparticles as highly active[1,4,5] and precious metal-free OER catalysts in alkaline solution. In this approach individual nanocatalysts are dispersed in an electrolyte solution and are electrically addressed during their Brownian motion-based impact at an inert microelectrode.[6–14] Applying a suitable potential, a steady-state catalytic current results at this nanocatalyst within microseconds[13,14] and a step-like increase in the current-time response is recorded (Figure 1).

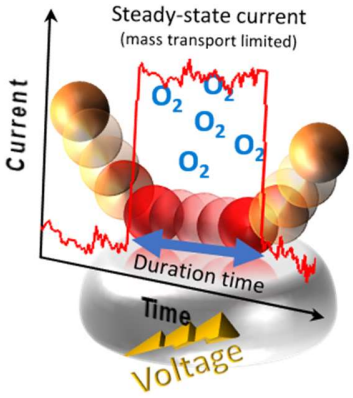

Figure 1. Nanoparticle OER impact illustration with steady-state current and duration.

While the step height depends on the particle size, its duration reflects the residence time of the catalyst at the electrode.[15] This enables us to measure the individual intrinsic catalytic response and to statistically evaluate the size distribution effects on electrocatalysts at the same time and without possible artefacts caused by additives or film porosity.[16]

Here we use this method to study the complex and industrially important OER in alkaline solution

$$4OH^- \rightleftarrows 2H_2O + O_2 + 4e^- \quad (1)$$

As a catalyst, Ø=4 nm sized spinel $CoFe_2O_4$ nanoparticles capped with triethyleneglycol are used as a proof-of-concept for the particle-by-particle assessment of nanocatalysts. $CoFe_2O_4$ nanoparticles were dispersed in 0.1 M KOH(aq) and the current response at a carbon microelectrode immersed into this suspension was recorded at a suitable potential of 1.86 V vs RHE (reversible hydrogen electrode). The obtained current-time response showed distinct current steps due to the catalytic OER at individual nanocatalyst particles during their sporadic impacts at the electrode (Figures 2 and 3).

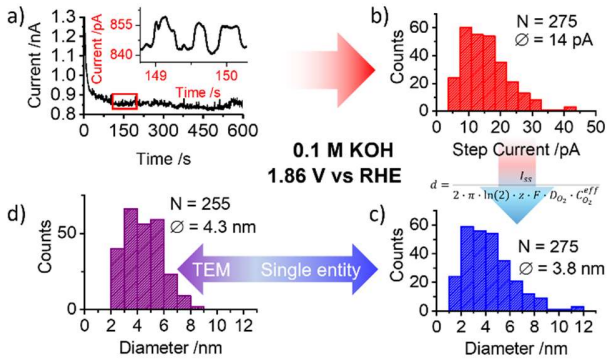

Figure 2: a) Chronoamperogram of 4 nm $CoFe_2O_4$ nanoparticles suspended in 0.1 M KOH(aq) recorded at 1.86 V vs RHE shows catalytic current steps (enlarged view in inset); b) histogram of step height (steady-state current) for 275 impacts; c) conversion of electrochemical step height distribution to particle size distribution[17] (see SI section S3 for details), shows good agreement with d) TEM (Figure S1).

The height of these current steps varied from about 4 pA to 30 pA, while the step duration varied from few milliseconds to several seconds. The distribution of the detected step heights, that is the distribution of the catalytic currents observed at individual nanocatalysts, reflects the inherent size distribution of the used $CoFe_2O_4$ nanocatalysts, as shown in Figures 2 and 3. Moreover, the values are in excellent agreement with those expected for a nanosphere in contact with an inert electrode, when the diffusional mass transport of the product limits the reaction.

$$I_{SS} = 2\pi \ln(2)\, zFD_{O_2}C_{O_2}^{eff} d \quad [18,19] \quad (2)$$

There I_{SS} is the steady-state catalytic current at the particle, (step height), z the number of transferred electrons (4 during OER), F the Faraday constant, D_{O_2} the diffusion coefficient and $C_{O_2}^{eff}$ the effective saturation concentration of oxygen in the electrolyte solution. Hence, a steady-state current of 15 pA is expected at a 4 nm particle in 0.1 M KOH at 25°C, where the diffusion coefficient and saturation concentration of oxygen are $D(O_2)=1.90\times10^{-9}$ m^2/s [20] and $C(O_2)=1.14$ mM (see SI S3.2.1), respectively.

Within the time scale of the experiment no agglomeration of $CoFe_2O_4$ nanoparticles was observed and the catalytic step heights remained constant during the experiment. Control experiments performed in the absence of catalyst particles and at lower particle concentrations, showed no and fewer impact features, respectively (Figure S8). Experiments at different applied potentials (Figure S7) confirm that the onset potential matches OER at $CoFe_2O_4$ nanoparticles and that the applied potential ensured mass transport limitation. Moreover, when agglomeration of $CoFe_2O_4$ nanoparticles was induced prior to the experiment, then significantly larger current steps resulted (Figure S8). This confirms that the recorded current steps are indeed caused by *individual* nanoparticles and that the size of the nanocatalysts limits the height of individual steps.

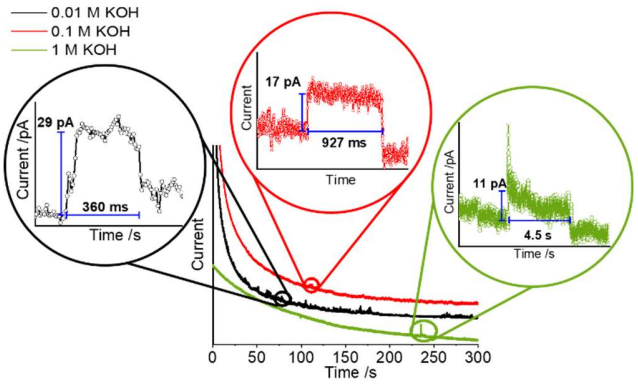

Figure 3: Chronoamperograms of $CoFe_2O_4$ nanoparticles suspended in different KOH(aq) concentrations: 0.01 M (black), 0.1 M (red) and 1.0 M (green); the graphs are vertically shifted for ease of comparison and example impact features are enlarged.

Experiments at different KOH concentrations verified that the catalytic steady-state current at individual $CoFe_2O_4$ nanoparticles is limited by removal of the product (O_2) and not by supply of reactant (OH^-) in strongly alkaline conditions. Current steps detected in 0.01 M, 0.1 M and 1.0 M KOH showed similar steady-state currents, in agreement with equation 2. This is due to the comparably similar solubility and diffusion coefficient of O_2 in all three electrolytes irrespective of the concentration of hydroxide being altered by two orders of magnitude.[20] If catalytic OER at a single 4 nm sized particle was limited by hydroxide, then step heights of about 0.35 nA, 3.5 nA and 35 nA would have resulted, respectively (see section S3 for details). To address the effect of the oxygen concentration on the step height, nano impact experiments were performed at

different O_2 concentrations. Figure 4a shows an absence of impact signals in oxygen-saturated suspensions (green), while in aerated (blue) and Ar-saturated (red) suspensions characteristic catalytic nano impact signals are observed. The absence of impact features in O_2-saturated suspensions and the scaling of their height with oxygen concentration further supports the conclusion that oxygen transport is the rate limiting process, while no significant supersaturation is detected (see S3.2.1).

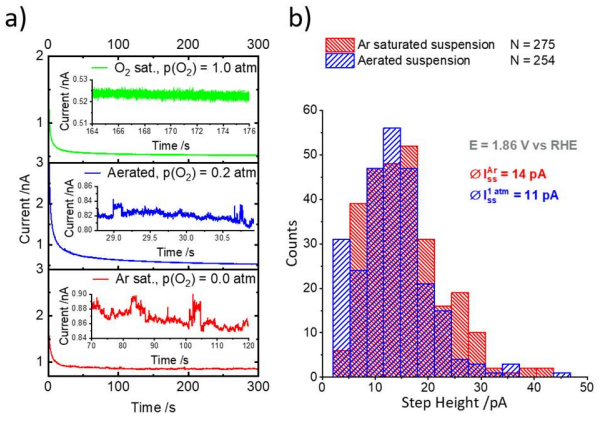

Figure 4: Effect of oxygen partial pressure p(O_2) on chronoamperometric impact experiments; a) step heights in oxygen-saturated (green), aerated (blue) and argon-purged (red) suspensions detected at 1.86 V vs RHE; insets show enlarged views. b) Step height histograms in aerated and Ar purged suspension show a ≈21 % shift of the mean values in agreement with the difference in oxygen concentration.

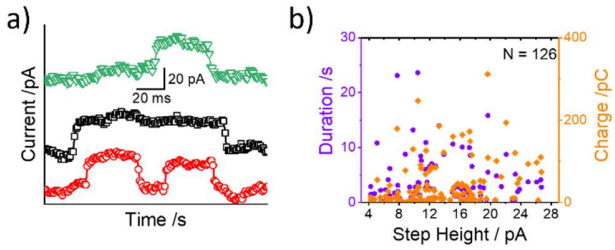

Figure 5: a) Examples of current steps of similar step height and different duration; b) plot of step duration (left y-axis, purple dots) and charge (right y-axis, orange rhombi) as function of step height show no relation.

The step duration is not an intrinsic feature of the impacting nanoparticle. It is a stochastic parameter that represents the random nature of nano impact events. Accordingly, steps of similar height (recorded at similarly sized particles) may differ strongly in duration, as shown in Figures 3 and 5a. Therefore, no correlation is seen when plotting the step duration as a function of the step height in Figure 4b (purple dots). This Figure also reveals that there is no correlation between the step height and the step area, that is, the charge passed per impact (orange rhombi). Hence, the amount of oxygen produced during an impact, is independent of the particle size. This suggests that indeed stochastic electrical disconnection of the particle due to its detachment from the electrode stops the catalytic OER at the nanocatalyst. Disconnection due to formation of an O_2 bubble is unlikely as it would scale with transferred charge and should yield a slowly decaying signal.[21]The sharp "on/off" transition of the current during the recorded steps and the plateauing step height further validate this conclusion. Catalytic impacts that are terminated due to catalyst poisoning would yield more gradual and triangular current spikes. Such response was reported recently for proton reduction at Pt nanoparticles[22]and for H_2O_2 oxidation at RuO_2 nanoparticles.[23]

Having demonstrated that catalytic OER at individual $CoFe_2O_4$ nanoparticles is detected, the current density at impacting particles can be identified to be in the order of tens to hundreds of kA·m^{-2}. This is an important achievement, as this is similar to industrially utilized current densities of several kA·m^{-2} [24,25], which is significantly bigger than the currents of few tens to hundreds of A·m^{-2} typically employed in academic research.

The $CoFe_2O_4$ nanoparticles employed in this work are crystalline and exhibit the spinel-type crystal structure, as confirmed by X-ray diffraction (Figure S3, PDF 1657817) and selected area electron diffraction measurements (SAED, Figures 6c,e).[26] Although $CoFe_2O_4$ nanoparticles are exposed to high overpotentials up to 1 V and very high current densities during linear sweep voltammetry OER (5 mV/s) herein, their spinel-type crystal structure is maintained after the electrochemical treatment. This is confirmed by bright-field TEM and SAED images before (Figure 6 a-c) and after (Figure 6 d-f) OER studies.

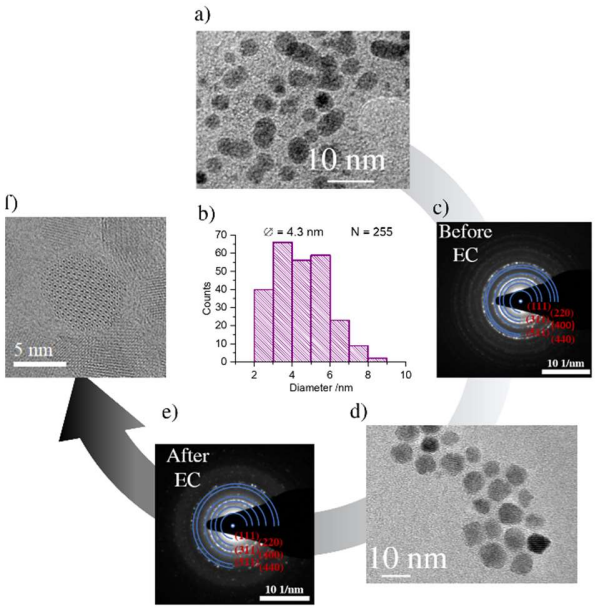

Figure 6: Bright-field TEM images and SAED studies of $CoFe_2O_4$ nanoparticles. a) TEM image, b) derived particle size distribution and c) SAED analysis before OER; d) TEM and e) SAED analysis after OER show no changes; f) HRTEM after OER shows intact spinel-type $CoFe_2O_4$ particles.

To easily compare the activity of the diverse range of homogeneous and heterogeneous catalysts, the turnover frequency (TOF) is a useful parameter. It relates the rate of product formation to the number of active sites of the catalyst. Using Faraday's law, the rate of oxygen formation during an impact ($n(O_2)$) is extracted from the recorded current step. Relating this to the number of Co ions at the particle surface $N(Co^{2+})$ yields the TOF:

$$TOF = \frac{I_{SS} \cdot N_A}{N(Co^{2+}) \cdot 4F}, \qquad (3)$$

where F is the Faraday- and N_A the Avogadro constant.

For example, an impacting 6.7 nm sized $CoFe_2O_4$ nanoparticle as shown in Figure S6 with a current step of 25 pA and N(Co^{2+})

= 157, yields a TOF of about 2.5x10^5 molecules of O_2 s^{-1}(see SI for details). This TOF is orders of magnitude larger than TOFs reported for state-of-the-art OER catalysts at supported nanoparticle films[25,27] and at enzymes (e.g. Photosystem II), where TOF values in the order of 10^3 O_2 s^{-1} or lower are typically reported.[28]

Note that despite the high current densities (kA·m^{-2}) and oxygen formation rates (≥10^5 O_2 molecules s^{-1}) obtained at individual $CoFe_2O_4$ nanocatalysts, the formation of oxygen (nano-)bubbles is unlikely, as due to that the small particle size and their spherical shape the nucleation of a bubble is hindred.[21,29,30] In line with that, no impact signals were detected in oxygen saturated suspensions (Figure 4a).

Exploiting electrocatalytic single nanoparticle studies, we demonstrate that the oxygen evolution reaction is mainly limited by removal of the product from the $CoFe_2O_4$ catalyst surface in strongly alkaline media. Varying the KOH concentration over three orders of magnitude verified that hydroxide concentration has no significant effect on the catalytic current. The electrochemically derived $CoFe_2O_4$ particle size distribution of 4±2 nm agreed very well with size distributions measured by TEM and AFM. Furthermore, SAED measurements of the used $CoFe_2O_4$ spinel particles showed no difference in crystal structure before and after the electrocatalysis experiments. This is true albeit very high current densities of several kA·m^{-2} are generated at these catalysts, which result in unprecedented turnover frequencies of >10^5 O_2 s^{-1} at these transition metal oxide catalysts. This does not only reveal the benefit of additive-free electrocatalyst evaluations. It also provides valuable new insights into the limiting factors governing OER at transition metal oxide catalysts in dependence of size, shape and activity. These insights are essential to identify structure-activity relations in these catalysts, which in turn are key to the rational design of affordable, highly active and stable electrocatalysts for future energy technologies.

ASSOCIATED CONTENT

Supporting Information

The Supporting Information is available free of charge on the ACS Publications website.

AUTHOR INFORMATION

Corresponding Author

Kristina.tschulik@ruhr-uni-bochum.de

Notes

The authors declare no competing financial interests.

ACKNOWLEDGMENT

The authors thank Prof Patrick Unwin (University of Warwick, UK) and Prof Martin Edwards (University of Utah, USA) for fruitful discussion and Dr. Dario Omanović (Ruđer Bošković Institute, Croatia) for providing „SignalCounter“ software. The authors acknowledge financial support by the Cluster of Excellence RESOLV (EXC-2033, #390677874) and Transregio (TRR247) funded by the German Research Foundation (DFG) and by the „NRW Rückkehrerprogramm“. A.E. acknowledges financial support by the Avicenna Studienwerk.

REFERENCES

(1) McCrory, C. C. L.; Jung, S.; Peters, J. C.; Jaramillo, T. F. Benchmarking heterogeneous electrocatalysts for the oxygen evolution reaction. *J. Am. Chem. Soc.* **2013**, *135*, 16977–16987.

(2) Kwon, S. J.; Fan, F.-R. F.; Bard, A. J. Observing iridium oxide (IrO(x)) single nanoparticle collisions at ultramicroelectrodes. *J. Am. Chem. Soc.* **2010**, *132*, 13165–13167.

(3) Masa, J.; Barwe, S.; Andronescu, C.; Sinev, I.; Ruff, A.; Jayaramulu, K.; Elumeeva, K.; Konkena, B.; Roldan Cuenya, B.; Schuhmann, W. Low Overpotential Water Splitting Using Cobalt–Cobalt Phosphide Nanoparticles Supported on Nickel Foam. *ACS Energy Lett.* **2016**, *1*, 1192–1198.

(4) Bian, W.; Yang, Z.; Strasser, P.; Yang, R. A $CoFe_2O_4$/graphene nanohybrid as an efficient bi-functional electrocatalyst for oxygen reduction and oxygen evolution. *J. Power Sources* **2014**, *250*, 196–203.

(5) Indra, A.; Menezes, P. W.; Sahraie, N. R.; Bergmann, A.; Das, C.; Tallarida, M.; Schmeisser, D.; Strasser, P.; Driess, M. Unification of catalytic water oxidation and oxygen reduction reactions: amorphous beat crystalline cobalt iron oxides. *J. Am. Chem. Soc.* **2014**, *136*, 17530–17536.

(6) Tschulik, K.; Cheng, W.; Batchelor-McAuley, C.; Murphy, S.; Omanović, D.; Compton, R. G. Non-Invasive Probing of Nanoparticle Electrostatics. *ChemElectroChem* **2015**, *2*, 112–118.

(7) Eloul, S.; Kätelhön, E.; Batchelor-McAuley, C.; Tschulik, K.; Compton, R. G. Diffusional Nanoimpacts: The Stochastic Limit. *J. Power Sources* **2015**, *119*, 14400–14410.

(8) Kwon, S. J.; Fan, F.-R. F.; Bard, A. J. Observing iridium oxide (IrO(x)) single nanoparticle collisions at ultramicroelectrodes. *J. Am. Chem. Soc.* **2010**, *132*, 13165–13167.

(9) Saw, E. N.; Kratz, M.; Tschulik, K. Time-resolved impact electrochemistry for quantitative measurement of single-nanoparticle reaction kinetics. *Nano Res.* **2017**, *129*, 3680–3689.

(10) Saw, E. N.; Blanc, N.; Kanokkanchana, K.; Tschulik, K. Time-resolved impact electrochemistry - A new method to determine diffusion coefficients of ions in solution. *Electrochim. Acta* **2018**, *282*, 317–323.

(11) Ahn, H. S.; Bard, A. J. Single-Nanoparticle Collision Events: Tunneling Electron Transfer on a Titanium Dioxide Passivated n-Silicon Electrode. *Angew. Chem. Int. Ed.* **2015**, *54*, 13753–13757.

(12) Kwon, S. J.; Zhou, H.; Fan, F.-R. F.; Vorobyev, V.; Zhang, B.; Bard, A. J. Stochastic electrochemistry with electrocatalytic nanoparticles at inert ultramicroelectrodes--theory and experiments. *Phys. Chem. Chem. Phys.* **2011**, *13*, 5394–5402.

(13) Sokolov, S. V.; Eloul, S.; Kätelhön, E.; Batchelor-McAuley, C.; Compton, R. G. Electrode-particle impacts: a users guide. *Phys. Chem. Chem. Phys.* **2016**, *19*, 28–43.

(14) Stevenson, K. J.; Tschulik, K. A materials driven approach for understanding single entity nano impact electrochemistry. *Curr. Opin. Electrochem.* **2017**, *6*, 38–45.

(15) Lin, C.; Compton, R. G. Size Effects in Nanoparticle Catalysis at Nanoparticle Modified Electrodes: The Interplay of Diffusion and Chemical Reactions. *J. Phys. Chem. C* **2017**, *121*, 2521–2528.

(16) Xiao, X.; Bard, A. J. Observing single nanoparticle collisions at an ultramicroelectrode by electrocatalytic amplification. *J. Am. Chem. Soc.* **2007**, *129*, 9610–9612.

(17) Ellison, J.; Tschulik, K.; Stuart, E. J. E.; Jurkschat, K.; Omanović, D.; Uhlemann, M.; Crossley, A.; Compton, R. G. Get more out of your data: A new approach to agglomeration and aggregation studies using nanoparticle impact experiments. *ChemistryOpen* **2013**, *2*, 69–75.

(18) Streeter, I.; Compton, R. G. Diffusion-Limited Currents to Nanoparticles of Various Shapes Supported on an Electrode; Spheres, Hemispheres, and Distorted Spheres and Hemispheres. *J. Phys. Chem. C* **2007**, *111*, 18049–18054.

(19) Bobbert, P. A.; Wind, M. M.; Vlieger, J. Diffusion to a slowly growing truncated sphere on a substrate. *Physica A: Statistical Mechanics and its Applications* **1987**, *141*, 58–72.
(20) Davis, R. E.; Horvath, G. L.; Tobias, C. W. The solubility and diffusion coefficient of oxygen in potassium hydroxide solutions. *Electrochim. Acta* **1967**, *12*, 287–297.
(21) Soto, Á. M.; German, S. R.; Ren, H.; van der Meer, D.; Lohse, D.; Edwards, M. A.; White, H. S. The Nucleation Rate of Single O2 Nanobubbles at Pt Nanoelectrodes. *Langmuir* **2018**, *34*, 7309–7318.
(22) Xiang, Z.-p.; Deng, H.-q.; Peljo, P.; Fu, Z.-y.; Wang, S.-l.; Mandler, D.; Sun, G.-q.; Liang, Z.-x. Electrochemical Dynamics of a Single Platinum Nanoparticle Collision Event for the Hydrogen Evolution Reaction. *Angew. Chem. Int. Ed.* **2018**, *57*, 3464–3468.
(23) Kang, M.; Perry, D.; Kim, Y.-R.; Colburn, A. W.; Lazenby, R. A.; Unwin, P. R. Time-Resolved Detection and Analysis of Single Nanoparticle Electrocatalytic Impacts. *J. Am. Chem. Soc.* **2015**, *137*, 10902–10905.
(24) Lu, X.; Zhao, C. Electrodeposition of hierarchically structured three-dimensional nickel-iron electrodes for efficient oxygen evolution at high current densities. *Nat. Commun.* **2015**, *6*, 6616.
(25) Burke, M. S.; Kast, M. G.; Trotochaud, L.; Smith, A. M.; Boettcher, S. W. Cobalt-iron (oxy)hydroxide oxygen evolution electrocatalysts: the role of structure and composition on activity, stability, and mechanism. *J. Am. Chem. Soc.* **2015**, *137*, 3638–3648.
(26) Chakrapani, K.; Bendt, G.; Hajiyani, H.; Lunkenbein, T.; Greiner, M. T.; Masliuk, L.; Salamon, S.; Landers, J.; Schlögl, R.; Wende, H.; Pentcheva, R.; Schulz, S.; Behrens M. The Role of Composition of Uniform and Highly Dispersed Cobalt Vanadium Iron Spinel Nanocrystals for Oxygen Electrocatalysis. *ACS Catal.* **2018**, *8*, 1259–1267.
(27) Xu, J.; Li, J.; Xiong, D.; Zhang, B.; Liu, Y.; Wu, K.-H.; Amorim, I.; Li, W.; Liu, L. Trends in activity for the oxygen evolution reaction on transition metal (M = Fe, Co, Ni) phosphide pre-catalysts. *Chem. Sci.* **2018**, *9*, 3470–3476.
(28) Ni, B.; Wang, K.; He, T.; Gong, Y.; Gu, L.; Zhuang, J.; Wang, X. Mimic the Photosystem II for Water Oxidation in Neutral Solution: A Case of Co_3O_4. *Adv. Energy Mater.* **2018**, *8*, 1702313.
(29) Wang, Y.; Hernandez, R. M.; Bartlett, D. J.; Bingham, J. M.; Kline, T. R.; Sen, A.; Mallouk, T. E. Bipolar electrochemical mechanism for the propulsion of catalytic nanomotors in hydrogen peroxide solutions. *Langmuir : the ACS journal of surfaces and colloids* **2006**, *22*, 10451–10456.
(30) Ren, H.; German, S. R.; Edwards, M. A.; Chen, Q.; White, H. S. Electrochemical Generation of Individual O_2 Nanobubbles via H_2O_2 Oxidation. *J Phys Chem Lett* **2017**, *8*, 2450–2454.

Insert Table of Contents artwork

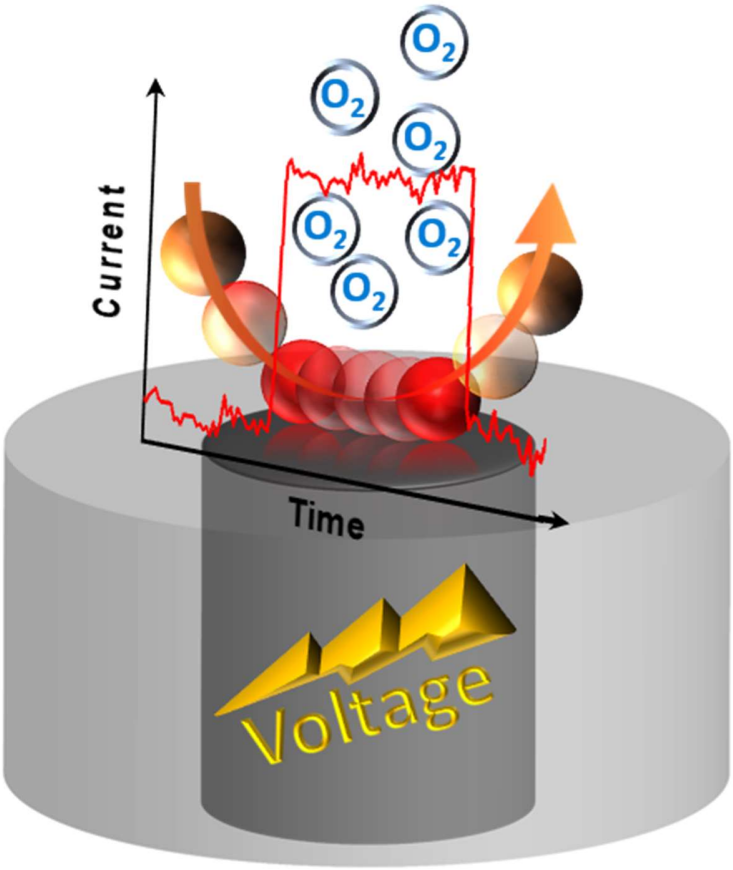

DOI: 10.1021/jacs.9b04516
URN: urn:nbn:de:hbz:464-20210127-145244-7